

## The effect of pre-annealing on the microstructure of (K,Na)NbO<sub>3</sub> ceramics

Sang Hwan Moon<sup>a</sup>, Jin Hong Choi<sup>a</sup>, Ki Woong Chae<sup>b</sup>, Jeog Seog Kim<sup>a</sup>, Chae Il Cheon<sup>a,b,\*</sup>

<sup>a</sup>Department of Semiconductor & Display Engineering, Hoseo University, Baebang, Asan, Chungnam 336-795, Republic of Korea

<sup>b</sup>Department of Materials Science & Engineering, Hoseo University, Baebang, Asan, Chungnam 336-795, Republic of Korea

Received 26 April 2012; received in revised form 27 August 2012; accepted 1 September 2012

Available online 11 September 2012

### Abstract

The effects of pre-annealing on the microstructure development and piezoelectric properties for 0.95(K<sub>0.5</sub>Na<sub>0.5</sub>)NbO<sub>3</sub>–0.05LiSbO<sub>3</sub> (0.95KNN–0.05LS) ceramics were investigated. The pre-annealing suppressed the abnormal grain growth in both the undoped and Mn-doped 0.95KNN–0.05LS ceramics. The pre-annealed samples possessed smaller abnormal grains, larger matrix grains, and a broader grain size distribution compared to the samples sintered without a pre-annealing step. The pre-annealed samples presented better dielectric and piezoelectric properties, a larger dielectric constant ( $\epsilon_r$ ) and electromechanical coupling factor ( $k_p$ ), and a smaller dielectric loss factor ( $\tan \delta$ ).

© 2012 Elsevier Ltd and Techna Group S.r.l. All rights reserved.

**Keywords:** A. Sintering; C. Piezoelectric properties; (K,Na)NbO<sub>3</sub>; Abnormal grain growth;

### 1. Introduction

Recently, lead-free piezoelectric ceramics have been researched in order to replace Pb(Zr,Ti)O<sub>3</sub>-based ceramics due to legislation regarding environmental restrictions. (K,Na)NbO<sub>3</sub>(KNN)-based ceramics have shown promising piezoelectric properties over the other lead-free piezoelectric compositions such as (Bi,Na)TiO<sub>3</sub>, Bi-layered structure ferroelectrics, etc. [1–3]. However, it has been reported that the preparation of KNN ceramic possessing a high density and an optimum microstructure through conventional ceramic processes is not easy, due to a severe volatilization of the alkali elements at high temperatures and/or cubic-shaped grain morphology [4,5]. There has been some advancement in enhancing the densities and piezoelectric properties of KNN ceramics by adding dopants such as Na<sub>2</sub>O, CuO and Li<sub>2</sub>O, which form liquid phases at low sintering temperature [6–10]. The ferroelectric properties of polycrystalline ceramics are dependent on the microstructure as

well as the density. There have been many reports regarding the dependence of the electrical properties on the microstructure in many piezoelectric ceramics such as BaTiO<sub>3</sub>, PbTiO<sub>3</sub>, Pb(Zr,Ti)O<sub>3</sub> and so on [11–14]. Although grain size control is very important in achieving high quality KNN-based ceramics, to date only a few studies on the grain growth behavior have been done regarding KNN-based ceramics.

When KNN-based ceramics are sintered at a high temperature in order to obtain a dense microstructure, an abnormal grain growth (AGG) has been frequently observed [4,6–12]. The AGG produces a bimodal grain size distribution and makes it difficult to control the microstructure and piezoelectric properties of the KNN ceramics [6–10]. Zhen et al. reported that the AGG was accelerated by the formation of a liquid phase and the volatilization of the alkali in Li/Ta-modified KNN ceramics [4,14]. AGGs have been observed above a certain temperature ( $T_{AGG}$ ) where an alkali volatilization is expected; the  $T_{AGG}$  was lowered when the liquid phase was formed by doping the ceramic with low-temperature melting additives [6–10].

AGGs have been reported to occur in materials with atomically faceted grain boundaries like KNN, and are

\*Corresponding author at: Department of Semiconductor & Display Engineering, Hoseo University, Baebang, Asan, Chungnam 336-795, Republic of Korea. Tel.: +82 41 540 5763; fax: +82 41 548 3502.

E-mail address: [cicheon@hoseo.edu](mailto:cicheon@hoseo.edu) (C.I. Cheon).

thought to be caused by 2-dimensional (2D) nucleation of steps on grains [6,7,15,16]. Fisher et al. reported that the reducing atmosphere during sintering caused a delay in the onset of the AGG and a reduction in the amount of the AGG in KNN ceramics [15]. They explained that the oxygen vacancies generated in the reducing atmosphere decreased the step free energy and thereby affected the grain growth behavior [15]. The decrease in the edge free energy reduced the critical driving force necessary for the 2D nucleation-controlled grain growth and changed the grain growth behavior from abnormal to pseudo-normal followed by abnormal growth [15]. Kim et al. also explained that the liquid phase reduced the critical driving force needed for a rapid growth of faceted grains and resulted in AGGs at low sintering temperatures in  $\text{Na}_2\text{O}$  or  $\text{Li}_2\text{O}$ -doped KNN ceramics [6,7].

Recently, dense ceramics with nano-sized grains have been successfully prepared using a two-step sintering process, in which the sample is first heated to a high temperature and then rapidly cooled and held at a lower temperature to make it fully dense [17,18]. Fang et al. demonstrated that by using this two-step sintering process a sound sintered density could be obtained in KNN-based ceramics over a wide sintering temperature range [19]. These KNN-based ceramics still had bimodal grain distributions. Their bimodal distribution indicated that AGG occurred during the first step, in which the sample was heated to a very high temperature for a very short time. Therefore, this two-step sintering process does not seem to be effective in the control of AGGs in KNN-based ceramics.

In this work, we attempted to suppress AGGs in KNN-based ceramics by adopting a different two-step sintering process from that presented by Fang et al. [17–19]. We pre-annealed  $0.95(\text{K}_{0.5}\text{Na}_{0.5})\text{NbO}_3\text{--}0.05\text{LiSbO}_3$  (0.95KNN–0.05LS) ceramic samples at a lower temperature than the final sintering temperature; the pre-annealing temperature was selected to be a little less than the AGG initiating temperature. 0.95KNN–0.05LS ceramics were also prepared by the normal sintering process without a pre-annealing step for comparison. The effects of the pre-annealing on the microstructure development and piezoelectric properties were then investigated.

## 2. Experimental

$\text{K}_2\text{CO}_3$  (High Pure Chemicals, 99%),  $\text{Na}_2\text{CO}_3$  (High Pure Chemicals, 99%),  $\text{Li}_2\text{CO}_3$  (High Pure Chemicals, 99%),  $\text{Nb}_2\text{O}_5$  (High Pure Chemicals, 99.9%), and  $\text{Sb}_2\text{O}_5$  (High Pure Chemicals, 99.9%) powders were weighed into the desired mole ratio, 0.95KNN–0.05LS and mixed by ball-milling for 16 h in plastic bottles with ethanol and yttria-stabilized zirconia (YSZ) balls. After drying, the mixed powder was calcined at 800 °C for 3 h and then at 950 °C for 3 h. The calcined powder was ball-milled again after adding 1 wt% polyvinyl butyral. 1 wt%  $\text{MnO}_2$  was added to the calcined powder in the Mn-doped 0.95KNN–0.05LS sample before ball-milling. The compacted 9 mm diameter disks were formed by uni-axial pressing and heat-treated at 600 °C for 5 h in order to burn-out the binder. The pressed samples were sintered using two different heating schedules: with and without pre-annealing. A group of samples were sintered at 1080–1100 °C for 3 h (the single-step sintering); the others were sintered at 1080–1100 °C for 3 h after pre-annealing them at 1060 °C for 3 h (the two-step sintering). All of the samples were heated at the rate of 200 °C/h and furnace-cooled. The phases of the calcined and sintered samples were identified using X-ray diffraction analysis (XD-D1; Shimadzu, Japan). The density of the sintered sample was measured by the Archimedes method. The surface morphologies were observed using a scanning electron microscope (Quanta 200, FEI).

Silver paste was printed onto the sintered samples and fired at 750 °C for 10 min for the electrical measurements. A 3 kV/mm electric field was applied to the samples for 10 min at 100 °C for dipole alignment, a process called poling. The dielectric properties of the samples were measured using an impedance analyzer (HP 4192 A). The ferroelectric P–E (polarization–electric field) hysteresis characteristics were analyzed using a ferroelectric tester (RT66A, Radiant Co.) and a high voltage amplifier (609E-6, Trek Co.). The piezoelectric constant  $d_{33}$  was measured using a Berlincourt-type  $d_{33}$  meter (YE2730A, APC International Ltd.).

## 3. Results

Fig. 1 shows the XRD patterns of (a) the undoped 0.95KNN–0.05LS and (b) the Mn-doped 0.95KNN–0.05LS

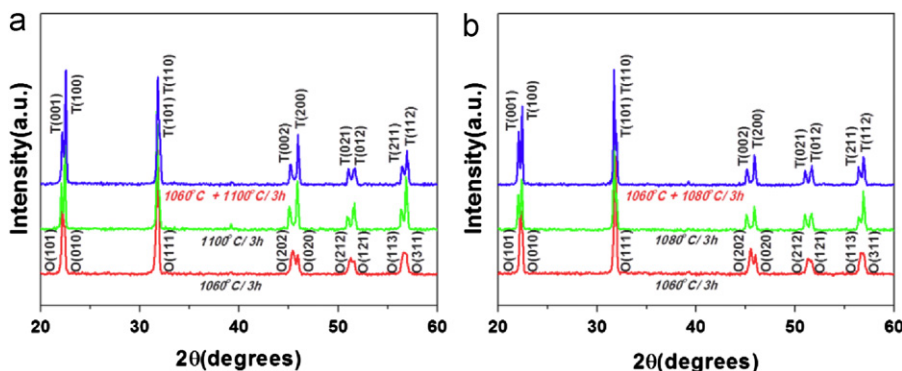


Fig. 1. The X-ray diffraction patterns of the (a) undoped and (b) Mn-doped 0.95KNN–0.05LS ceramics.

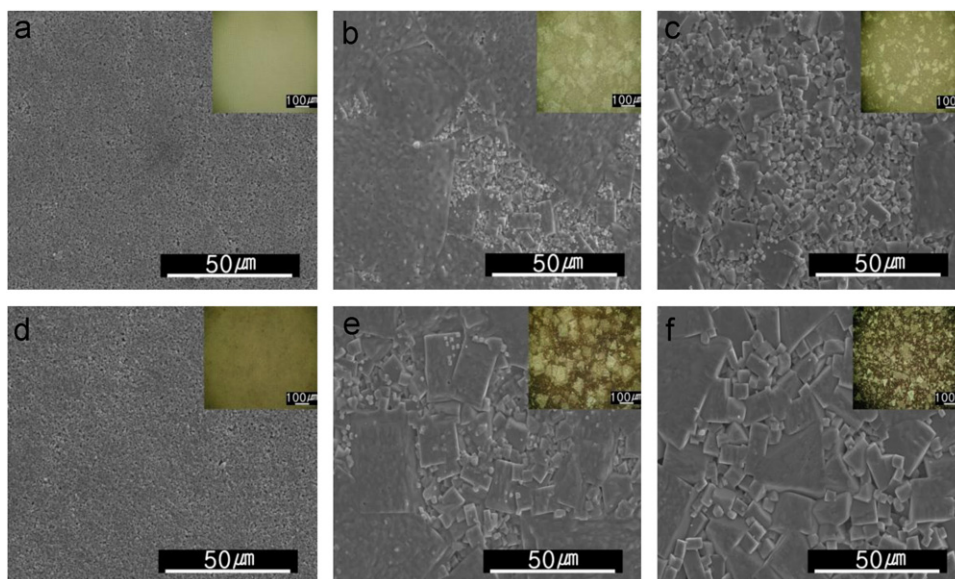


Fig. 2. The surface morphologies of the undoped 0.95KNN–0.05LS ceramics sintered (a) at 1060 °C for 3 h, (b) at 1100 °C for 3 h, and (c) at 1100 °C for 3 h after pre-annealing at 1060 °C for 3 h and the Mn-doped ceramics sintered (d) at 1060 °C for 3 h, (e) at 1080 °C for 3 h, and (f) at 1080 °C for 3 h after pre-annealing at 1060 °C for 3 h.

samples. The XRD patterns of the conventionally sintered samples and the two-step processed samples were compared. The undoped samples seen in Fig. 1(a) were sintered using either conventional sintering conditions (1060 °C and 1100 °C) or the two-step processing (pre-annealing at 1060 °C for 3 h and sintering at 1100 °C for 3 h). The Mn-doped samples in Fig. 1(b) were also sintered by using either the conventional sintering method (at 1060 °C and at 1080 °C for 3 h) or the two-step sintering process (pre-annealed at 1060 °C and then sintered at 1080 °C for 3 h). The morphotropic phase boundary (MPB) composition of the KNN-LS ceramic was found to be about 0.948KNN–0.052LS; the crystal structure was orthorhombic at an LS content smaller than the MPB composition and tetragonal for an LS content larger than the MPB [20,21]. As shown in Fig. 1, a single perovskite phase was observed without any impurity phase in both the undoped and Mn-doped 0.95KNN–0.05LS ceramics. The crystal structure of the undoped 0.95KNN–0.05LS sample was orthorhombic when sintered at 1060 °C for 3 h and changed to tetragonal when sintered at 1100 °C for 3 h, both with and without the pre-annealing step. In the Mn-doped samples the crystal structure also changed from orthorhombic to tetragonal at the sintering temperature of 1080 °C, as shown in Fig. 1(b). This crystal structure change from orthorhombic at the low sintering temperature to tetragonal at the high sintering temperature has been reported and claimed to result from the compositional change due to the volatilization of alkali metal oxides during high temperature sintering [19,22,23]. The composition of this work, 0.95KNN–0.05LS is very near to the reported MPB composition of 0.948KNN–0.052LS. Therefore, the crystal structure change in Fig. 1 seems to be caused by the evaporation of the Na and/or K which results in an increase in the Li/(K + Na + Li) ratio.

The surface morphologies of the undoped 0.95KNN–0.05LS and Mn-doped 0.95KNN–0.05LS ceramics are shown in Fig. 2. The insets present optical micrographs at a low magnification. The undoped 0.95KNN–0.05LS ceramic sintered at 1060 °C seen in Fig. 2(a) displays a uniform microstructure with a small grain size of less than 1 μm. Large grains at around 100 μm, however, are observed in the small matrix grains when sintered at 1100 °C as shown in Fig. 2(b). This is a typical microstructure caused by abnormal grain growth (AGG) and has been reported in many KNN-based ceramics [4,6–12]. The AGG is also observed in the sample sintered at 1100 °C for 3 h after pre-annealing at 1060 °C for 3 h, however it is less severe compared to that sintered at 1100 °C for 3 h without a pre-annealing step, as shown in Fig. 2(c). Fig. 2(b) and (c) demonstrate that the pre-annealing reduced both the number and average size of the abnormal grains. The undoped 0.95KNN–0.05LS sample sintered with a pre-annealing step had larger matrix grains and a broader grain size distribution compared to the sample sintered without a pre-annealing step. A uniform microstructure possessing small grains of less than 1 μm is also observed in the Mn-doped 0.95KNN–0.05LS ceramic sintered at 1060 °C, as shown in Fig. 2(d). Fig. 2(e) and (f) shows that AGG occurred in the Mn-doped samples sintered at 1080 °C both with and without the pre-annealing step. Just as found in the undoped 0.95KNN–0.05LS sample, the Mn-doped sample with the pre-annealing step showed smaller abnormally grown grains, larger matrix grains, and a broader grain size distribution compared to the sample without a pre-annealing step.

The properties of the 0.95KNN–0.05LS ceramics are listed in Table 1. The samples with the pre-annealing step have larger densities, which indicate that the pre-annealing

Table 1  
Properties of the undoped and Mn-doped 0.95KNN–0.05LS ceramics.

Composition	Sintering condition	Density (g/cm <sup>3</sup> )	Dielectric constant at 1 MHz	Dielectric loss (tan $\delta$ ) at 1 MHz	Electromechanical coupling factor, $k_p$
Undoped 0.95KNN–0.05LS	1100 °C/3 h	4.189	821	0.064	0.332
	1060 °C/3 h + 1100 °C/3 h	4.314	1084	0.044	0.396
Mn-doped 0.95KNN–0.05LS	1080 °C/3 h	4.378	974	0.036	0.398
	1060 °C/3 h	4.416	1084	0.034	0.406
	+ 1080 °C/3 h				

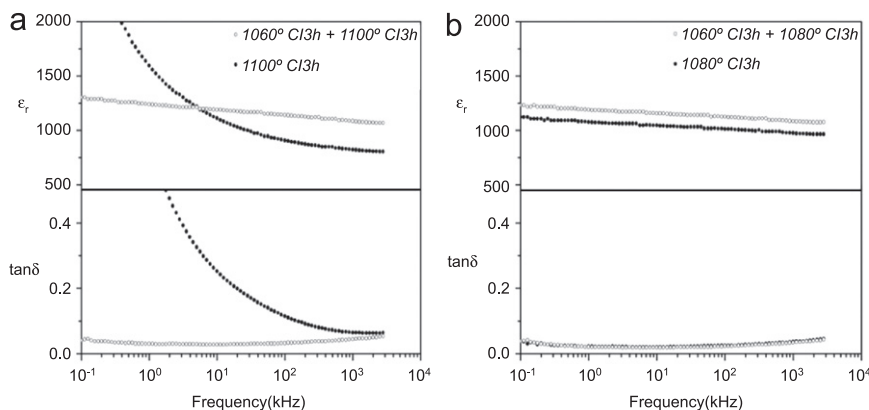


Fig. 3. The dielectric properties of the (a) undoped and (b) Mn-doped 0.95KNN–0.05LS ceramics.

improved the densification. As shown in Fig. 2 and Table 1, the Mn-doped 0.95KNN–0.05LS ceramic sintered at 1080 °C had larger matrix grains and larger densities than the undoped ceramics sintered at 1100 °C, even though the sintering temperature of the Mn-doped ceramic was lower by 20 °C. The temperature for the AGG onset was lower by about 20 °C in the Mn-doped 0.95KNN–0.05LS ceramic compared to the undoped sample. The addition of MnO<sub>2</sub> or MnO has been reported to facilitate grain growth and densification, and thereby lower the temperature needed for densification and abnormal grain growth in KNN-based ceramics [24,25].

The dielectric and ferroelectric properties of the 0.95KNN–0.05LS ceramics are illustrated in Figs. 3 and 4, respectively. Fig. 3(a) illustrates that the dielectric constant and loss rise with the decrease in the measuring frequency in the undoped 0.95KNN–0.05LS ceramic at 1100 °C (single-step sintering) whereas the sample employing the pre-annealing step (two-step sintering) has stable frequency characteristics for the dielectric constant and loss. However, stable frequency characteristics for the dielectric constant and loss are shown in the Mn-doped samples sintered both with and without a pre-annealing step (Fig. 3(b)). The undoped 0.95KNN–0.05LS ceramic sintered at 1,100 °C (single-step sintering) had a leaky ferroelectric P–E hysteresis loop. The sample employing the pre-annealing step had a well-saturated P–E hysteresis loop, as shown in Fig. 4(a). Fig. 4(b) demonstrates a well-saturated P–E hysteresis loop in the Mn-doped samples both with and without a pre-annealing step. The samples

with a pre-annealing step also had better dielectric and piezoelectric properties as shown in Table 1, i.e. a larger dielectric constant ( $\epsilon_r$ ) and electromechanical coupling factor ( $k_p$ ), and a smaller dielectric loss factor (tan  $\delta$ ). The enhancement of the electrical properties by pre-annealing was slight in the Mn-doped sample compared to the undoped sample.

#### 4. Discussion

It has been reported that ceramics with faceted grain boundaries like KNN-based ceramics develop abnormal grain growth through two-dimensional (2D) nucleation and growth during liquid phase sintering [6,7,15,16,26]. The AGG has been reported to be closely related to the formation of the interfacial liquid phase [4,6–10,14–16,26–28]. The formation of the interfacial liquid phase has been reported in KNN-based ceramics by a partial melting at the temperature above the solid–liquid phase line in KNN-based ceramics [28]. And the melting temperature is around 1100 °C in KNN with Na/K = 50/50 and depends on the exact composition of KNN-based ceramics [28].

The uniform grain distributions observed in the pre-annealed samples, as shown in Fig. 2(a) and (d), indicate that the normal grain growth occurred during the pre-annealing. Many abnormally grown grains appeared abruptly only by a temperature increase of 20–40 °C above the pre-annealing temperature as shown in Fig. 2. Therefore, the AGGs observed in this work also seem to be facilitated by the formation of the liquid phase during the



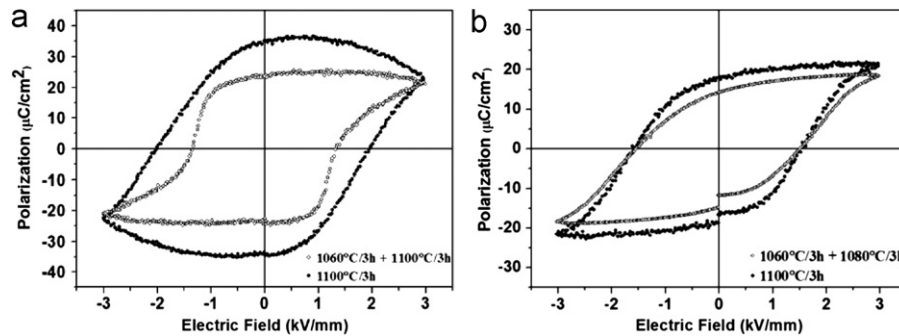


Fig. 4. The ferroelectric P–E hysteresis loops of the (a) undoped and (b) Mn-doped 0.95KNN–0.05LS ceramics.

final sintering process. Fig. 2 demonstrates that the pre-annealing at 1060 °C for 3 h inhibited the AGG. It decreased the number and the size of the abnormal grains while increasing the average size of the matrix grain in both the undoped and Mn-doped 0.95KNN–0.05LS ceramics. The suppression of the AGG by the pre-annealing is thought to be caused by the reduction in the driving force given due to overall grain growth during the pre-annealing process. It is worth emphasizing that the pre-annealing temperature should be a little below the liquid phase formation temperature for the suppression of the AGG. The reduction of the AGG amount has been observed when the KNN ceramics were sintered in a reducing atmosphere [15]. However, sintering in a strongly reducing atmosphere would produce KNN ceramics with a low resistivity due to the great number of ionic defects. The pre-annealing process in air could be an effective method to suppress the AGG without losing insulating resistance in KNN-based ceramics.

Mn-doping is known to facilitate the grain growth and densification of KNN-based ceramics [24,25]. Manganese has been reported to replace the B site ions and generate oxygen vacancies for charge neutrality in  $\text{ABO}_3$  perovskite compounds like  $\text{BaTiO}_3$  and  $\text{Pb}(\text{Zr,Ti})\text{O}_3$  [29]. A similar effect is also observed in Fig. 2 and Table 1. It is considered that the Mn-doping reduces the AGG onset temperature and increases the density and matrix grain size due to the decrease of the liquid formation temperature and the generation of oxygen vacancies.

The undoped 0.95KNN–0.05LS ceramic sintered at 1100 °C without the pre-annealing step displays a high dielectric loss at low frequencies and a leaky P–E hysteresis loop, as shown in Figs. 3 and 4(a). A high dielectric loss at 1 kHz and a leaky P–E hysteresis loop have also been observed in KNN-based ceramics sintered at a low temperature, they also had a low density and a very small grain size [30]. The porous matrix region with very small grains in the undoped sample without the pre-annealing step might lead to a high dielectric loss at low frequencies, the leaky P–E hysteresis loop, and the poorer piezoelectric properties seen in Table 1. The matrix region with the larger grains and denser microstructure in the undoped 0.95KNN–0.05LS ceramic sintered at 1100 °C

after pre-annealing might give the stable frequency characteristics in the dielectric properties. The Mn-doped 0.95KNN–0.05LS ceramic sintered at 1080 °C demonstrates a stable dielectric property and a well saturated P–E hysteresis loop even when sintered without a pre-annealing step, as shown in Figs. 3 and 4(b). This is because the sample has larger matrix grains and a denser microstructure which is indicated by the larger density shown in Table 1. The Mn-doping has been reported to reduce the dielectric loss in KNN-based ceramics [24] and the Mn-doping in this work also seems to have a role to improve the dielectric and ferroelectric properties. The dielectric and piezoelectric properties are enhanced by pre-annealing in both the undoped and Mn-doped 0.95KNN–0.05LS ceramics probably due to the higher density and larger matrix grain size, as shown in Table 1.

## 5. Conclusion

An abnormal grain growth was observed in both the undoped and Mn-doped 0.95KNN–0.05LS ceramics sintered at 1080 °C and 1100 °C, respectively. Pre-annealing at 1060 °C for 3 h before the sintering suppressed the abnormal grain growth in both undoped and Mn-doped 0.95KNN–0.05LS ceramics. The pre-annealed samples showed a lesser degree of abnormal growth behavior, i.e. larger matrix grains and a broader grain size distribution than that found for the samples sintered without the pre-annealing step. The Mn-doped 0.95KNN–0.05LS ceramics had larger matrix grains, higher densities and lower onset temperature for the abnormal grain growth than the undoped ceramics. The pre-annealed samples have better dielectric and piezoelectric properties: a larger dielectric constant ( $\epsilon_r$ ) and electromechanical coupling factor ( $k_p$ ), and a smaller dielectric loss factor ( $\tan\delta$ ). The pre-annealing is an effective process that improves electrical properties as well as suppresses abnormal grain growth in 0.95KNN–0.05LS ceramics.

## Acknowledgment

This research was supported by the Academic Research fund of Hoseo University in 2009 (2009-0043).

## References

- [1] Y. Saito, H. Takao, T. Tani, T. Nonoyama, K. Takatori, T. Homma, T. Nagaya, M. Nakamura, Lead-free piezoceramics, *Nature* 432 (2004) 84–87.
- [2] T.R. Shrout, S.J. Zhang, Lead-free piezoelectric ceramics: alternatives for PZT?, *Journal of Electroceramics* 19 (2007) 111–124.
- [3] Y. Gao, J. Zhang, Y. Qing, Y. Tan, Z. Zhang, X. Hao, Remarkably strong piezoelectricity of lead-free  $(\text{K}_{0.45}\text{Na}_{0.55})_{0.98}\text{Li}_{0.02}(\text{Nb}_{0.77}\text{Ta}_{0.18}\text{Sb}_{0.05})\text{O}_3$  ceramic, *Journal of the American Ceramic Society* 94 (2011) 2968–2973.
- [4] Y. Zhen, J.F. Li, Normal sintering of  $(\text{K},\text{Na})\text{NbO}_3$ -based ceramics: influence of sintering temperature on densification, microstructure, and electrical properties, *Journal of the American Ceramic Society* 89 (2006) 3669–3675.
- [5] C.W. Ahn, C.S. Park, C.H. Choi, S. Nahm, M.J. Yoo, H.G. Lee, S. Priya, Sintering behavior of lead-free  $(\text{K},\text{Na})\text{NbO}_3$ -based piezoelectric ceramics, *Journal of the American Ceramic Society* 92 (2009) 2033–2038.
- [6] M.S. Kim, D.S. Lee, E.C. Park, S.J. Jeong, J.S. Song, Effect of  $\text{Na}_2\text{O}$  additions on the sinterability and piezoelectric properties of lead-free  $95(\text{Na}_{0.5}\text{K}_{0.5})\text{NbO}_3$ – $5\text{LiTaO}_3$  ceramics, *Journal of the European Ceramic Society* 27 (2007) 4121–4124.
- [7] M.S. Kim, S.J. Jeong, J.S. Song, Microstructures and piezoelectric properties in the  $\text{Li}_2\text{O}$ -Excess  $0.95(\text{Na}_{0.5}\text{K}_{0.5})\text{NbO}_3$ – $0.05\text{LiTaO}_3$  ceramics, *Journal of the American Ceramic Society* 90 (2007) 3338–3340.
- [8] H.Y. Park, C.W. Ahn, K.H. Cho, S. Nahm, H.G. Lee, H.W. Kang, D.H. Kim, K.S. Park, Low-temperature sintering and piezoelectric properties of  $\text{CuO}$ -added  $0.95(\text{Na}_{0.5}\text{K}_{0.5})\text{NbO}_3$ – $0.05\text{BaTiO}_3$  ceramics, *Journal of the American Ceramic Society* 90 (2007) 4066–4069.
- [9] I.T. Seo, H.Y. Park, N.V. Dung, M.K. Choi, S. Nahm, H.G. Lee, B.H. Choi, Microstructure and piezoelectric properties of  $(\text{Na}_{0.5}\text{K}_{0.5})\text{NbO}_3$  lead-free piezoelectric ceramics with  $\text{V}_2\text{O}_5$  addition, *IEEE Transactions on Ultrasonics, Ferroelectrics, and Frequency Control* 56 (2009) 2337–2342.
- [10] K. Wang, J.F. Li, Low-temperature sintering of Li-modified  $(\text{K},\text{Na})\text{NbO}_3$  lead-free ceramics: sintering behavior, microstructure, and electrical properties, *Journal of the American Ceramic Society* 93 (2010) 1101–1107.
- [11] M. Kahn, Influence of grain growth on dielectric properties of Nb-doped  $\text{BaTiO}_3$ , *Journal of the American Ceramic Society* 54 (1971) 455–457.
- [12] J.A. Perez, M.R. Soares, P.Q. Mantas, A.M.R. Senos, Microstructural design of PZT ceramics, *Journal of the European Ceramic Society* 25 (2005) 2207–2210.
- [13] L.A. Celi, A.C. Caballero, M. Villegas, J. Defrutos, J.F. Fernandez, Effect of grain growth control on PZT properties, *Ferroelectrics* 270 (2002) 105–110.
- [14] Y. Zhen, J.F. Li, Abnormal grain growth and new core-shell structure in  $(\text{K},\text{Na})\text{NbO}_3$ -based lead-free piezoelectric ceramics, *Journal of the American Ceramic Society* 90 (2007) 3496–3502.
- [15] J.G. Fisher, S.J.L. Kang, Microstructural changes in  $(\text{K}_{0.5}\text{Na}_{0.5})\text{NbO}_3$  ceramics sintered in various atmosphere, *Journal of the European Ceramic Society* 29 (2009) 2581–2588.
- [16] C. Wang, Y.D. Hou, H.Y. Ge, M.K. Zhu, H. Yan, Growth of  $(\text{Na}_{0.5}\text{K}_{0.5})\text{NbO}_3$  single crystal grain growth method from special shaped nano-powders, *Journal of the European Ceramic Society* 30 (2010) 1725–1730.
- [17] I.-W. Chen, X.-H. Wang, Sintering dense nanocrystalline ceramics without final-stage grain growth, *Nature* 404 (2000) 168–171.
- [18] X.-H. Wang, P.-L. Chen, I.-Wei Chen, Two-step sintering of ceramics with constant grain-size, I.  $\text{Y}_2\text{O}_3$ , *Journal of the American Ceramic Society* 89 (2006) 431–437.
- [19] J. Fang, X. Wang, Z. Tian, C. Zhong, L. Li, Two-step sintering: an approach to broaden the sintering temperature range of alkaline niobate-based lead-free piezoceramics, *Journal of the American Ceramic Society* 93 (2010) 3552–3555.
- [20] S. Zhang, R. Xia, T.R. Shrout, G. Zang, J. Wang, Piezoelectric properties in perovskite  $0.948(\text{K}_{0.5}\text{Na}_{0.5})\text{NbO}_3$ – $0.052\text{LiSbO}_3$  lead-free ceramics, *Journal of Applied Physics* 100 (2006) 104108.
- [21] J. Wua, D. Xiao, Y. Wang, J. Zhu, P. Yu, Y. Jiang, Compositional dependence of phase structure and electrical properties in  $(\text{K}_{0.42}\text{Na}_{0.58})\text{NbO}_3$ – $\text{LiSbO}_3$  lead-free ceramics, *Journal of Applied Physics* 102 (2007) 114113.
- [22] P. Zhao, B.P. Zhang, J.F. Li, High piezoelectric  $d_{33}$  coefficient in Li-modified lead-free  $(\text{Na},\text{K})\text{NbO}_3$  ceramics sintered at optimal temperature, *Applied physics letters* 90 (2007) 242909.
- [23] K. Wang, J.F. Lee, Domain engineering of lead-free Li-modified  $(\text{K},\text{Na})\text{NbO}_3$  polycrystals with highly enhanced piezoelectricity, *Advanced Functional Materials* 20 (2010) 1924.
- [24] D. Lin, K.W. Kwok, H. Tian, H.W.L. Chan, Phase transitions and electrical properties of  $(\text{Na}_{1/3}\text{K}_x)(\text{Nb}_{1/3}\text{Sb}_y)\text{O}_3$  lead-free piezoelectric ceramics with a  $\text{MnO}_2$  sintering aid, *Journal of the American Ceramic Society* 90 (2007) 1458–1462.
- [25] P. Bomlai, P. Sinsap, S. Muensit, S.J. Milne, Effect of  $\text{MnO}$  on the phase development, microstructures, and dielectric properties of  $0.95\text{Na}_{0.5}\text{K}_{0.5}\text{NbO}_3$ – $0.05\text{LiTaO}_3$  ceramics, *Journal of the American Ceramic Society* 91 (2008) 624–627.
- [26] W. Jo, D.-Y. Kim, N.-M. Hwang, Effect of interface structure on the microstructural evolution of ceramics, *Journal of the American Ceramic Society* 89 (2006) 2369–2380.
- [27] Rohrer Gregory S., Influence of interface anisotropy on grain growth and coarsening, *Annual Review Of Materials Research* 35 (2005) 99–126.
- [28] J. Fang, X. Wang, R. Zuo, Z. Tian, C. Zhong, L. Li, Narrow sintering temperature window for  $(\text{K},\text{Na})\text{NbO}_3$ -based lead-free piezoceramics caused by compositional segregation, *Physica Status Solidi A* 208 (2011) 791–794.
- [29] Y. Xu, *Ferroelectric Materials and Their Applications*, Elsevier Science Publishers, B. V., Amsterdam, The Netherlands, 1991 136–138.
- [30] J. Fang, X. Wang, L. Li, Properties of ultrafine-grained  $\text{Na}_{0.5}\text{K}_{0.5}\text{NbO}_3$  ceramics prepared from nanopowder, *Journal of the American Ceramic Society* 94 (2011) 1654–1656.